University of Regensburg

Fortgeschrittenenpraktikum

Experiment: Pockels-Effekt

Trainees: Erik Fabrizzi, Fabian Tanzer

28. June 2021

Contents

1 Preparation

This experiment investigates the change in optical birefringence when an electric field is applied. If this relationship is linear, it is also referred to in physics as the Pockels effect. This effect is used, for example, in optical switches (Pockels cells) or in laser Q-switching (Q-switching).

1.1 Often used physical quantities

For better readability, commonly used quantities are listed here once:

n:	Refractive index
n_o bzw. $n_\perp$:	Refractive index of the ordinary ray
n_e bzw. $n_{\vert\vert}$:	Refractive index of the extraordinary ray
v_o bzw. $v_\perp$:	Wave velocity of the ordinary ray
v_e bzw. $v_{\vert\vert}$:	Wave velocity of the extraordinary ray

1.2 Electro-optic effect

The dependence of the refractive index n on an external electric field E is called **elekcro-optic effect**:

$$n(E) = n_0 + S_1 E + S_2 E^2 + ... \tag{1}$$

where n_0 is the refractive index in the absence of an electric field:

$$n_0 = n(E = 0) \tag{2}$$

1. case: $S_1 \neq 0$: linear electro-optic effect (**Pockels effect**)
The change of the birefringence is therefore linear to the change of the electric field E.

2. case: $S_1 = 0$ und $S_2 \neq 0$: quadratic electro-optic effect (**Kerr effect**)
Thus, the change in birefringence is quadratic to the change in electric field E.
In this experiment the 1st case is treated. It occurs due to nonlinearities[1] in optically nonlinear[2] crystals.
The following figure provides an overview of frequently used terms:

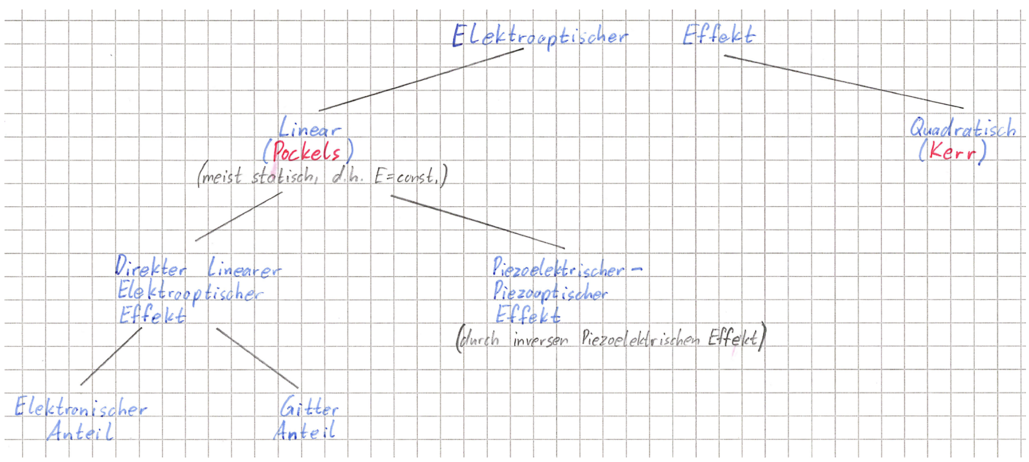

Fig. 1: Overview of the relationship between different electro-optical effects. (self created)

[1] also causes frequency doubling of laser light, stimulated Raman scattering from optical phonons
[2] risk of confusion with linear dependence of refractive index on electric field E

1.3 Piezoelectric effect

The piezoelectric effect (in short: piezoelectric effect) describes the relationship between mechanical stress and electrical surface charges in solids. A distinction is made between the following types:

- direct piezoelectric effect:
  Mechanical stresses occur during the deformation of solids. Microscopic dipoles are formed within the elementary cells due to the displacement of the centers of charge. The summation over all elementary cells of the crystal leads to a macroscopically measurable electrical stress. As a result, electric charges are generated on the surface of certain materials. [1, p.18]
- inverse piezoelectric effect:
  When electric voltage, i.e., an external electric field, is applied, the ions in each unit cell are displaced by electrostatic forces in such a way that the entire crystal deforms. [1, p.18]

1.4 Crystals without inversion center

The Pockels effect does not occur in crystals with inversion center.

Proof: Consider crystal with inversion center. Since the refractive index n changes linearly with the applied electric field E in the Pockels effect, the following applies:

$$\Delta n = k \cdot E \qquad \text{with } k \in \mathbb{R} \tag{3}$$

If the electric field is now reversed to $\tilde{E}$, the following holds:

$$\tilde{E} = -E \tag{4}$$

Due to the inversion symmetry of the crystal:

$$\Delta \tilde{n} = \Delta n \tag{5}$$

So it follows:

$$\begin{aligned} &\Delta n = \Delta \tilde{n} \\ \Leftrightarrow\ &k \cdot E = k \cdot \tilde{E} \\ \Leftrightarrow\ &k \cdot E = -k \cdot E \\ \Leftrightarrow\ &\Delta n = -\Delta n \\ \Leftrightarrow\ &\Delta n = 0 \end{aligned} \tag{6}$$

So there is no refractive index change. □

Thus, the Pockels effect occurs, for example, with ammonium dihydrogen phosphate ($NH_4H_2PO_4$, abbreviated ADP), lithium niobate ($LiNbO_3$), gallium arsenide (GaAs), or potassium dihydrogen phosphate (KD_2PO_4, abbreviated KD*P).

In addition, these crystals also show the piezoelectric effect (s. 1.5.2).

1.5 Pockels effect

The static linear electrooptic effect is generated by constant electric fields and includes two parts. It is therefore valid

$$r_{ijk} = r'_{ijk} + r^{p}_{ijk} \tag{7}$$

1.5.1 Direct linear electrooptic effect r'_{ijk}

The direct linear electrooptic effect is immediately visible when an electric field is applied. It is again composed of two components:

- Electronic fraction:
  Results from the deformation of the electron shells when exposed to the electric field.
- Lattice fraction:
  Caused by the relative shifts of the positive ionic lattice with respect to the negative one.

1.5.2 Piezoelectric piezo-optical additional contribution r^p_{ijk}

If an electric voltage and thus electric field is applied to a crystal, the crystal is deformed (inverse piezoelectric effect). This results in displacements of the negative and the positive ion lattice in phase [2, p. 2]. As a result, the refractive index changes. The deformation gives rise to relief waves which propagate in the crystal at the speed of sound v_s. These reach the measuring point after the time

$$t = \frac{d}{v_\mathrm{s}} \tag{8}$$

where
d: Distance of the measuring point from surface
v_s: Speed of sound in crystal

Thus, in contrast to the direct electro-optical effect the piezoelectric-piezo-optical additional contribution becomes only visible with a time delay in the form of elastic relief waves in the impulse response [2, p. 1].

1.6 Isotropic vs. anisotropic

In optically isotropic media, the electric field $\vec{E}$ is perpendicular to the wave vector $\vec{k}$. Thus, a plane is already defined in which the $\vec{E}$ field can oscillate. Moreover, isotropic media have a refractive index independent of direction. Isotropy occurs primarily in gases, liquids, and amorphous solids [3]. Concrete examples are glass and crystals with cubic lattice structure. When light passes through optically anisotropic matter, its polarization state usually changes. In the case of anisotropic media, a further distinction is made between **uniaxial** (e.g. calcite and quartz) and **biaxial**. Anisotropy leads to directional refractive index (ordinary refractive index n_o and extraordinary refractive index n_e), resulting in **birefringence**. Thus, a **optical axis**[3] exists.

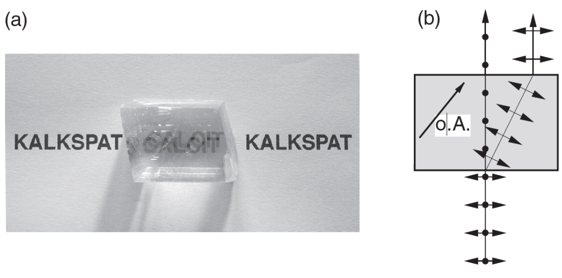

Fig. 2: a) Photo of the birefringence on a calcite crystal. b) Illustration of different transmission pathways (ordinary and extraordinary ray) [4]

[3] along the o. A. (optical axis), each polarization component of a light beam experiences the same refractive index. Thus, no birefringence occurs along the o. A.

If $\Delta n = n_e - n_o < 0$, the crystal is said to be **negative birefringent**. According to the consideration

$$\begin{aligned} &\Delta n < 0 \\ \Leftrightarrow\ & n_e < n_o \\ \Leftrightarrow\ & \frac{c}{v_e} < \frac{c}{v_o} \\ \Leftrightarrow\ & v_e > v_o \end{aligned} \tag{9}$$

the extraordinary beam moves faster than the ordinary beam.

If $\Delta n = n_e - n_o > 0$, the crystal is called **positive birefringent** (e.g. quartz). Analogous to the above consideration, the extraordinary ray moves slower than the ordinary ray.

1.7 Polarization states

One can write any plane wave as:

$$\vec{E} = \vec{E_x} + \vec{E_y} \tag{10}$$

$$= E_{x0}\cos(\omega t - kz) + E_{y0}\cos(\omega t - kz + \psi) \tag{11}$$

This results in the following possible polarization states ($n \in \mathbb{N}$):

- linearly polarized: $E_{x0} = E_{y0}$ and $\psi = n\pi$
- circularly polarized: $E_{x0} = E_{y0}$ and $\psi = \left(n + \frac{1}{2}\right)\pi$
- elliptical polarized: else

The following figure illustrates how the respective polarization states are composed.

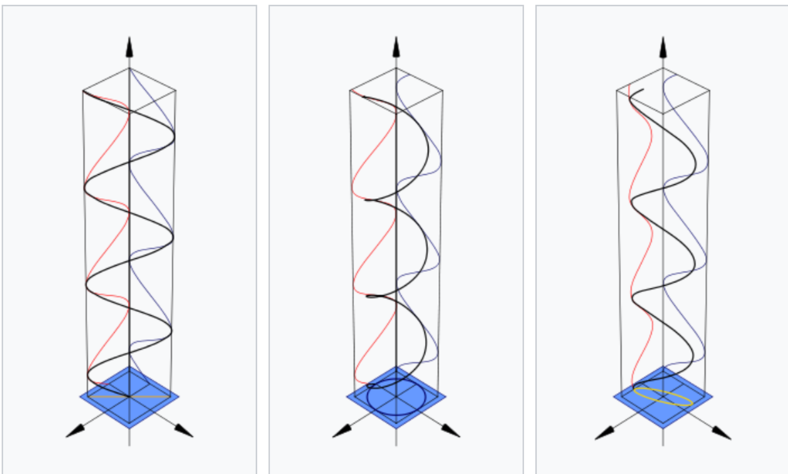

Fig. 3: Composition of a linearly, circularly or elliptically polarized wave (black) from linearly polarized components (red and blue) [5]

1.8 Measurement

Problem: When measuring with static fields (i.e. constant electric field strength E), the distinction between direct linear electrooptic effect and piezoelectric-piezooptic additional contribution is not possible.

Solution: Therefore, short rectangular voltage pulses are applied to the crystal. This causes the birefringence ratios in the crystal to change. This is made visible with the aid of a laser beam, recorded via a photodiode and displayed on an oscilloscope. This leads to images similar to those in Fig. 4.

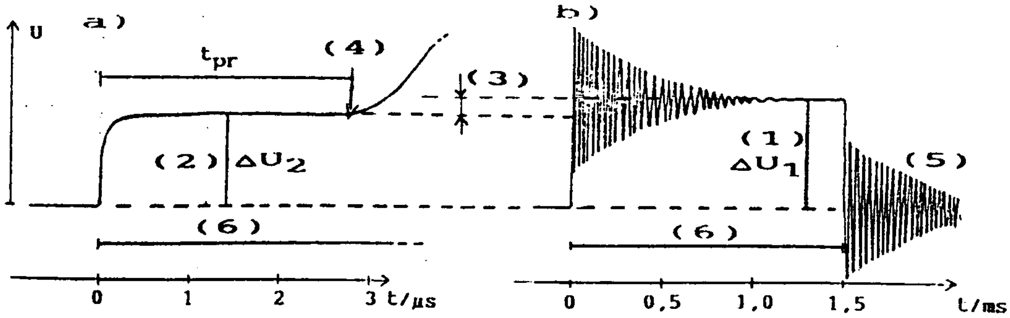

Fig. 4: Impulse response.
a) Initial phase of the impulse response (time resolution greater by a factor of 500 than in b), but same amplitude scale.
b) total impulse response
(1) static linear electrooptic effect
(2) direct linear electrooptic effect
(3) piezoelectric piezo-optical additional contribution
(4) delayed arrival of the relief waves
(5) piezoelectric disturbance
(6) temporal expansion of the voltage pulse

Now for the description of fig. 4:
It should be noted that a) represents only a very small initial part of b). As described in 1.5.1, the electronic and the lattice part of the direct linear electrooptic effect (2) is formed immediately with the onset of the voltage pulse. The piezoelectric-piezo-optic additional contribution (3) becomes visible only with a time delay t_{pr} (4). The deformation gives rise to relief waves that run from the edge into the crystal and propagate at the speed of sound in the crystal [2, p. 2]. After multiple reflections, the waves are attenuated away at the crystal surface. If the pulse length was sufficient, the crystal is then homogeneously deformed. The static linear electro-optical effect (1) is thus achieved. The end of the pulse (6) now causes a piezoelectric-piezooptical effect (5) again.

1.9 Pockels cell

The Pockels cell used in this experiment consists essentially of a KD*P crystal. Since a longitudinal arrangement[4] should be present, two electrodes are attached to the crystal in a ring shape:

[4]longitudinal arrangement: laser beam in the direction of the electric field vector $\vec{E}$,
transversal arrangement: laser beam perpendicular to the electric field vector $\vec{E}$

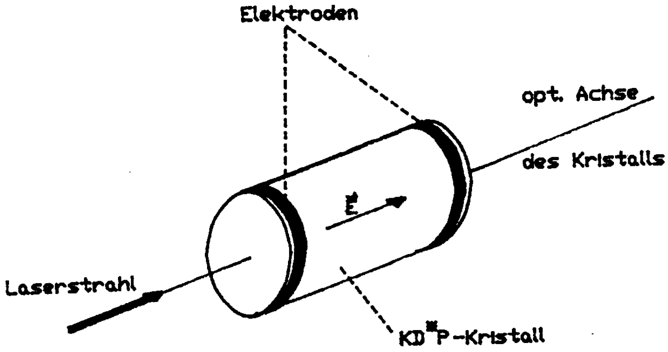

Fig. 5: Pockels cell made of KD*P with vapor-deposited electrodes in longitudinal arrangement

The KD*P crystal is **optically uniaxial**, i.e. it has exactly one optical axis.
Since the refractive index n_e of the extraordinary beam is smaller than the refractive index n_o of the ordinary beam

$$1,46 = n_\mathrm{e} < n_\mathrm{o} = 1,51 \tag{12}$$

the KD*P crystal is **negative birefringent**. According to 1.6, the extraordinary light wave propagates faster in the crystal than the ordinary light wave:

$$v_\mathrm{e} > v_\mathrm{o} \tag{13}$$

<u>Without electric field E:</u>
No birefringence occurs when the laser beam passes through the crystal parallel to the o. A.

<u>With electric field E:</u>
Laser beam is split into two linear polarized partial waves perpendicular to each other. These partial waves have different propagation velocities in the crystal (see (9)), which leads to a phase shift δ between the partial waves:

$$\frac{\delta}{2\pi} = \frac{\Delta n l}{\lambda} \qquad \Leftrightarrow \qquad \delta = 2\pi \Delta n \frac{l}{\lambda} \tag{14}$$

where

- δ: Phase difference of two mutually perpendicularly polarized partial waves
- l: Crystal length
- λ: Wavelength of the laser light

This phase difference δ is determined by means of the senarmont compensator.

1.10 Glan-Taylor polarizer

The **Glan-Taylor prism** is a polarizer based on birefringence and total internal reflection that linearly polarizes unpolarized light:

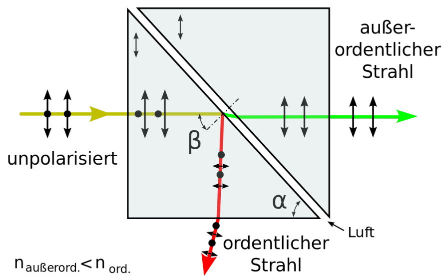

Fig. 6: Structure of a Glan-Taylor prism [6]

It consists of a birefringent crystal (usually calcite). The entrance and exit surfaces are parallel to the o. A. The crystal is cut into two parts in such a way that the refractive index difference between ordinary and extraordinary beam causes a different reflection behavior (i.e. total reflection and transmission) at the interface to the air gap. A sufficiently thick air gap remains between the two crystal parts to prevent transmission into the second prism by total internal reflection.
Compared to the **Nicol's prism**, the Glan-Taylor prism is approximately a cube and thus shorter.

1.11 Senarmont method

The Senarmont method can be used to measure the optical phase difference of two linearly polarized partial waves perpendicular to each other. Laser, polarizer (Glan-Taylor polarizer, see 1.10), Pockels cell, $\frac{\lambda}{4}$-plate and an analyzer are needed.

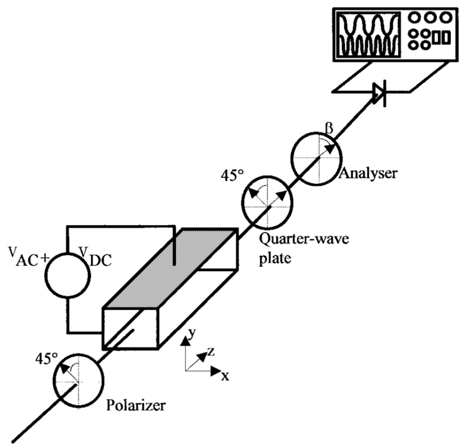

Fig. 7: Structure for the Senarmont method [7]

If a voltage U is applied to the Pockels cell, the light is elliptically polarized after passing through the Pockels cell. The main oscillation axis of the quarter-wave plate is to be adjusted so that the elliptically polarized light coming from the Pockels cell is linearly polarized after passing. Its polarization direction is rotated by the angle α with respect to the original polarization direction of the laser light. The angle α is reached when a minimum of the light intensity is reached. This can be read as a DC voltage signal on the oscilloscope. The phase difference is then

$$\delta = 2\alpha \tag{15}$$

1.12 Representation of the birefringence ratio

There are two ways to illustrate the birefringence ratios in a crystal: The normal index ellipsoid[5] and the optical index ellipsoid.

1.12.1 Normal index ellipsoid

The refractive indices n_o and n_e are both plotted in the direction of propagation of the incident light wave. This results in a sphere for the ordinary ray and an ellipsoid[6] for the extraordinary ray, which are usually represented one inside the other as a bivalve figure [2, p. 3].

1.12.2 Optical index ellipsoid (relevant here)

Here n_o and n_e are plotted in a plane perpendicular to the direction of propagation of light (i.e., to the wave vector $\vec{k}$):

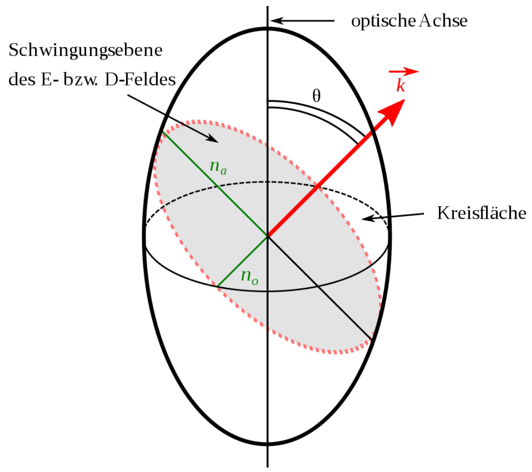

Fig. 8: Index ellipsoid of an optically uniaxial crystal (rotational ellipsoid) [8]

From the **general Dupin indicatrix equation**

$$\sum_{ij} \left(\frac{1}{n^2}\right)_{ij} \tilde{x}_i \tilde{x}_j = 1 \tag{16}$$

the equation describing the resulting (single-shell) figure is obtained by principal axis transformation:

$$\frac{x_1^2}{n_1^2} + \frac{x_2^2}{n_2^2} + \frac{x_3^2}{n_3^2} = 1 \tag{17}$$

For the KD*P crystal, the indicatrix has the form of a rotational ellipsoid[7]. Its rotation axis is the o. A. of the crystal. Since KD*P is optically uniaxial, applies:

$$n_1 = n_2 = n_\mathrm{o} \qquad \text{and} \qquad n_3 = n_\mathrm{e} \tag{18}$$

[5] **index ellipsoid:** Dupin indicatrix, which is used to calculate the birefringence

[6] **Ellipsoid:** 3-dimensional equivalent of an ellipse. Affine image of unit sphere with equations in cartesian coordinates: $\frac{x^2}{a^2} + \frac{y^2}{b^2} + \frac{z^2}{c^2} = 1$ with $a, b, c > 0$

[7] **rotational ellipsoid:** a=b, so $\frac{x^2+y^2}{a^2} + \frac{z^2}{c^2} = 1$ with $a, b > 0$

and thus

$$\frac{x_1^2 + x_2^2}{{n_\mathrm{o}}^2} + \frac{x_3^2}{{n_\mathrm{e}}^2} = 1 \tag{19}$$

The coordinate axes of the index ellipsoid coincide with those of the crystal coordinate system such that the crystallographic c-axis (o. A) corresponds to the x_3-axis of the indicatrix.

1.13 Calculation of r_{63}

The coefficient r_{63} stands abbreviatively for r_{123} or r_{213} (see **usual index abbreviation**).
In the script it is deduced that the birefringence induced by the electric field E is

$$\Delta n = r_{63} E_3 n_\mathrm{o}^3 \tag{20}$$

From electrodynamics it is known that when a voltage U is applied to a crystal of crystal length l, an electric field

$$E = \frac{U}{l} \tag{21}$$

results.
So we know that for the searched coefficient r_{63} the following relationship is valid:

$$\begin{aligned} r_{63} &\overset{(20)}{=} \frac{\Delta n}{E_3 n_\mathrm{o}^3} \\ &\overset{(14)}{=} \frac{\delta\lambda}{2\pi l E_3 n_\mathrm{o}^3} \\ &\overset{(21)}{=} \frac{\delta\lambda l}{2\pi l n_\mathrm{o}^3 U} \\ &= \frac{\delta\lambda}{2\pi U n_\mathrm{o}^3} \qquad (22) \\ &\overset{(15)}{=} \frac{\alpha\lambda}{\pi U n_\mathrm{o}^3} \qquad (23) \end{aligned}$$

Since the crystal length l truncates out, the wavelength λ of the laser, the applied voltage U, and n_o are known, the coefficient r_{63} can now be easily calculated.

2 Experimental Results

2.1 Calibration

Before starting the experiment we set up the experiment by ensuring that all optical components that needed to be used in the experiment were working and aligned.
The calibration of the setup was executed as follows:

1. Analyzer is set perpendicular to the polarizer which can be found the beginning of the light path. This is achieved by turning the analyzer until a complete cancellation of the beam is achieved.
2. A $\frac{\lambda}{4}$-Plate is added in the light path between analyzer and polarizer and gets adjusted until complete cancellation of the beam is achieved, meaning that the optical axis of the $\frac{\lambda}{4}$-Plate is parallel to the polarizer axis.
3. The $\frac{\lambda}{4}$-Plate is now removed from the light path and the Pockels cell is inserted and driven on DC. It is placed in the optical path and a short focal length lens is mounted directly in front of it to expand the laser beam. The cell position gets then adjusted so that the beam passes centrally through the cell and any reflections are minimized. If this is the case, a so-called isogyrene cross is created on the screen, which should have its maximum exactly in the center of the screen.

2.2 Impulse Response

In the first part of the experiment the Pockels-cell will be driven with 50 % Duty Cicle PWM (Pulse-width modulation) signal at high voltage. The output of the laser will be then measured by a photo-diode at the end of the light path and analyzed whit the help of an oscilloscope.
The main goal of this experiment is determine how the birefringence of the crystal develops with time after an electric field is been applied to it.
This time dependence is related to the speed of the relaxation waves in the crystal that are already been discussed in chapter 1.5.

2.2.1 Measure results and determination of sound velocity in crystal

As one can clearly see in the oscilloscope output the impulse response follows the expected Development. The relaxation waves takes about $t_r = 2.320$ µs to reach the measuring point. Using the relationship between velocity and relaxation delay of equation 8 we are able to determine the sound velocity in the crystal:

$$v_{\mathrm{s}} = \frac{x_{\mathrm{eff}}}{2t_{\mathrm{r}}} = \frac{d_{\mathrm{cell}} - d_{\mathrm{beam}}}{2t_r} = 1.5 \cdot 10^3 \, \frac{\mathrm{m}}{\mathrm{s}} \tag{24}$$

where:
x_{eff} is the effective distance from measuring point to contact point.
d_{cell} and d_{beam} are the cell diameter of 7 mm and beam diameter of 1 mm.

The measured velocity is sufficiently close to the theoretical value of $1.60 \cdot 10^3 \, \frac{\mathrm{m}}{\mathrm{s}}$.

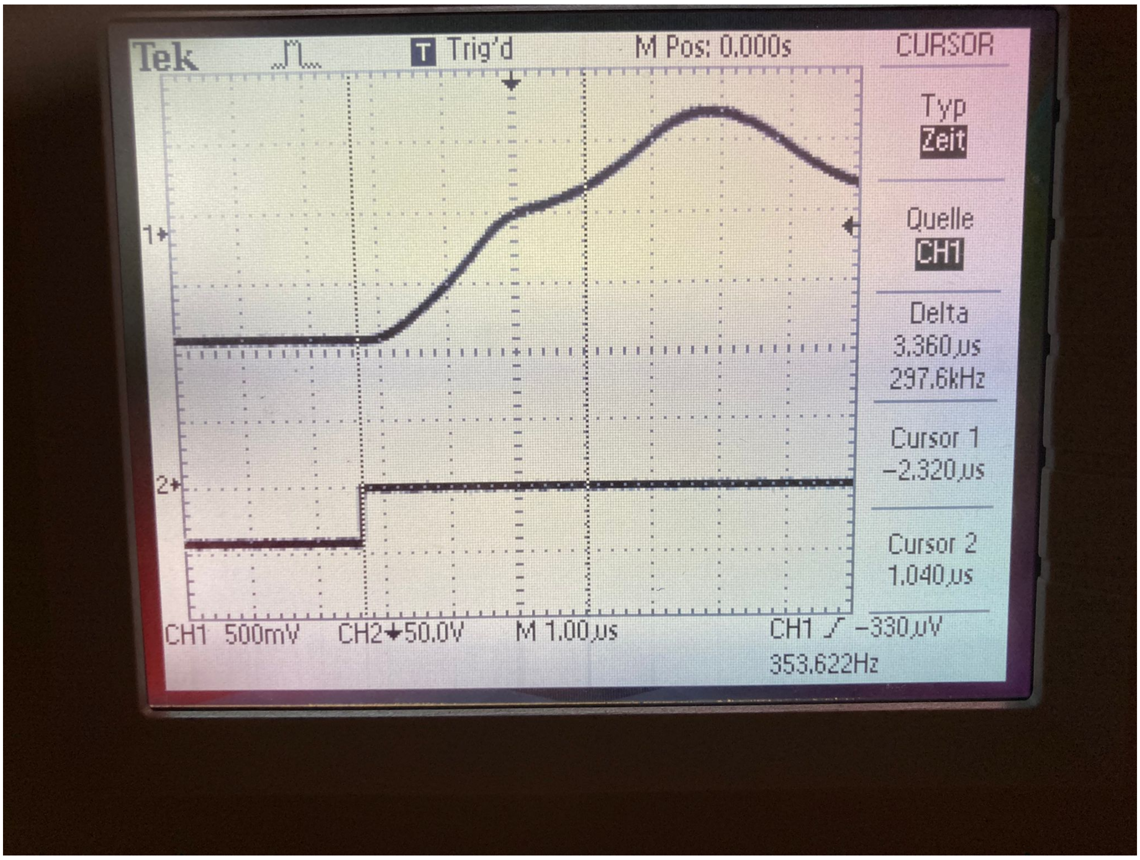

Fig. 9: Intensity of laser at detector (top curve) and driving voltage (bottom curve) as displayed by the oscilloscope (Voltage against time). The displayed vertical lines mark the two points for the relaxation time measurement which is displayed on the right column on screen. The x-axis shows the time in microseconds.

2.2.2 Influence of Piezoeletric effect and Elctro-optical effect on the measure

In this section we will discuss the relationship between the two main components of the Pockels effect. Such measurement can be done considering that the change in amplitude observed in the oscilloscope is linearly proportional to the the constants of the static electrooptic effect r_{63} and that of the direct linear electrooptical effect r'_{63}.
Therefore:

$$\frac{r'_{63}}{r_{63}} = \frac{U_1}{U_2} = \frac{0,78}{1} = 0,78 \tag{25}$$

This result is really interesting since it allows us to understand that most of the effect ($\approx 80\,\%$) is directly depending on the electro-optical effect.

2.3 Measuring r_{63}: Senarmont Method and wavelength dependency

In the second part of the experiment the Senarmont method was used to determine the coefficient r_{63} for two different wavelenghts: 632 nm and 820 nm. To proceed with the measurements the pre-adjusted $\frac{\lambda}{4}$-plate was added to the light path and the Pockels-cell has been driven with an high DC voltage ranging from -1500 to 1500 volts. The magnitude of the DC voltage could be adjusted on the supply.

2.3.1 Execution

As already discussed in the theoretical introduction to this experiment, (particularly in section 1.13) we can determine r_{63} by searching for minima of the intensity at the detector by adjusting the analyzer. A zero reference was set by turning off the power supply and adjusting the analyzer until the light at detector was canceled. After powering the Pockels-cell the next minima was manually determined by adjusting the analyzer and measured with respect to the zero reference.

2.4 Calculating r_{63}

As we already saw in section 1.13, particularly in equation 23, we know that for:

$$\alpha = k_{\text{lin}} U = \frac{n_0^3 \pi r_{63}}{\lambda} U \tag{26}$$

where k_{lin} is the slope of a linear fit on the measured data. Therefore:

$$r_{63} = \frac{k_{\text{lin}} \lambda}{n_0^3 \pi} \tag{27}$$

since we measured the angles in degrees we will use $\pi = 180°$.

2.4.1 Experimental results for $\lambda = 632$ nm

We achieved really good experimental results whit the 632 nm Laser: The sampled points are clearly linearly depended to voltage with very little error except for some point near the zero. From our prospective this errors have no physical meaning and are a consequence of a not really precise measure of the analyzer´s angle .

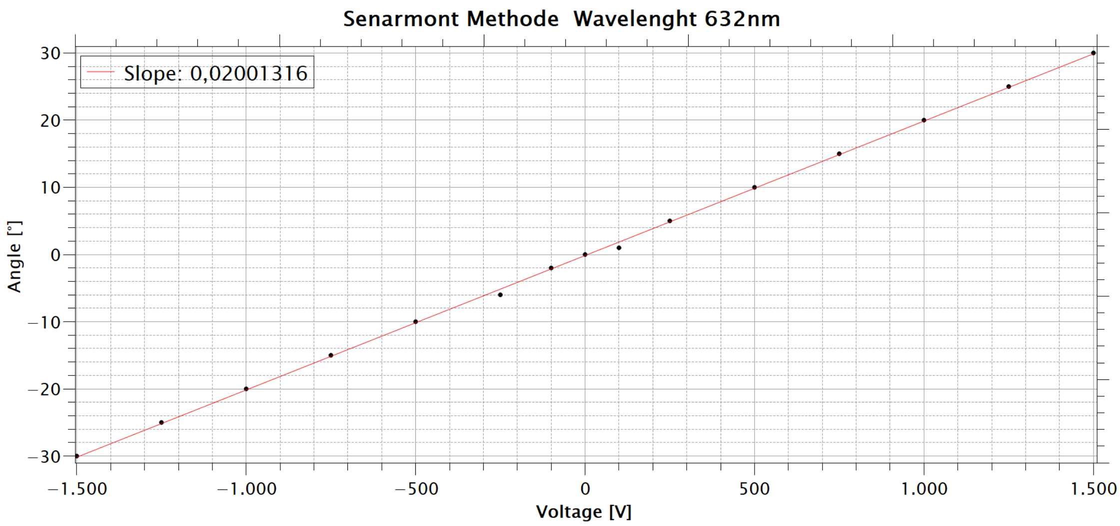

Fig. 10: Plot of angle of intensity minimum vs voltage in Senarmont Method for HeNe laser with a wavelength of 632 nm, slope value of linear fit is displayed in the legend. The x-axis shows the voltage in volts. The y-axis shows the angle in degrees.

Using equation 27 with pulse-width modulation literature value for n_0 of 1,53 we obtain:

$$r_{63} = 2,08 \cdot 10^{-11} \, \frac{\text{m}}{\text{V}} \tag{28}$$

Which agrees with the theoretical value of $2,33 \cdot 10^{-11} \frac{\text{m}}{\text{V}}$. For r'_{63}, using the results of the previous section, we obtain:

$$r'_{63} = 0,78\,\frac{\mathrm{m}}{\mathrm{V}},\ r_{63} = 1.622 \cdot 10^{-11}\,\frac{\mathrm{m}}{\mathrm{V}} \tag{29}$$

2.4.2 Experimental results for $\lambda = 820$ nm

The measures with the 820 nm laser were also successfully. It is to note that the $\frac{\lambda}{4}$-Plate was substituted whit an appropriate one for the new wavelength. The sampled points display some slightly non linear behavior witch, since the seam to be symmetric with respect to the 0, may be dependent on some second order terms of the electro-optical effect. A linear approximation seems to still be appropriate for the Pockels-cell used in the experiment.

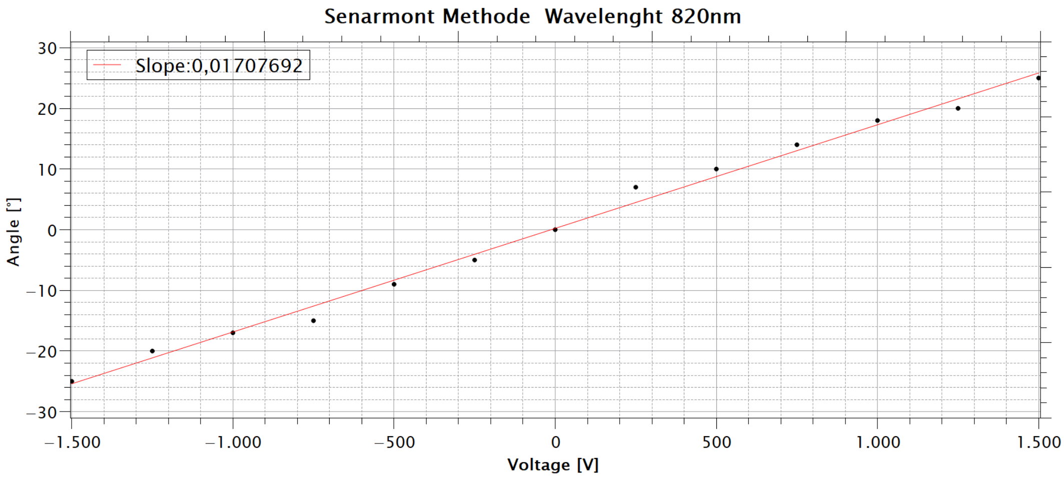

Fig. 11: Plot of angle of intensity minimum vs voltage in Senarmont Method for Infrarot laser with a wavelength of 820 nm, slope value of linear fit is displayed in the legend. The x-axis shows the voltage in volts. The y-axis shows the angle in degrees.

Using again equation 27 with literature given value for n_0 of 1,53 we obtain:

$$r_{63} = 2,29 \cdot 10^{-11}\,\frac{\mathrm{m}}{\mathrm{V}} \tag{30}$$

and for r'_{63}:

$$r'_{63} = 0,78\,\frac{\mathrm{m}}{\mathrm{V}},\ r_{63} = 1.79 \cdot 10^{-11}\,\frac{\mathrm{m}}{\mathrm{V}} \tag{31}$$

3 Conclusion

In conclusion we have measured in experiment the Pockels effect, which is a linear-optical effect. We applied electric field to a crystal and measured the refractive index. We quantified the birefringence of the KPD crystal. The Impulse Response worked very well, we nearly reached the theoretical value. In the part, where we calculated r_{63} the results are also good. We used different wavelength and in each part we could show the linear dependence. So all in all we can say that the experimental results match well with the theoretical forecasts.

List of Figures

References

[1] G. Kern, *Rastertunnelmikroskopie - Aufbau eines neuen Versuchs für das Fortgeschrittenen-praktikum (Zulassungsarbeit).* Universität Regensburg, 2008.

[2] *Der lineare elektrooptische Effekt (Pockels-Effekt).* Universität Regensburg, Oct. 1991.

[3] Spektrum Akademischer Verlag, "Isotropie," https://www.spektrum.de/lexikon/physik/isotropie/7595, Heidelberg, (Accessed 26.06.2021).

[4] W. Zinth and U. Zinth, *Optik, Lichtstrahlen-Wellen-Photonen*, ser. 4., aktualisierte Auflage. München: Oldenbourg Verlag, 2013.

[5] Wikipedia, die freie Enzyklopädie, "Polarisation," https://de.wikipedia.org/wiki/Polarisation, 2021, (Accessed 26.06.2021).

[6] ——, "Glan-Taylor-Prisma," https://de.wikipedia.org/wiki/Glan-Taylor-Prisma, 2021, (Accessed 26.06.2021).

[7] L. Guilbert, J. P. Salvestrini, H. Hassan, and M. D. Fontana, "Combined Effects Due to Phase, Intensity, and Contrast in Electrooptic Modulation: Application to Ferroelectric Materials," https://ieeexplore.ieee.org/document/748830/authors#authors, Mar. 1999, (Accessed 27.06.2021).

[8] Wikipedia, die freie Enzyklopädie, "Indexellipsoid," https://de.wikipedia.org/wiki/Indexellipsoid, 2021, (Accessed 26.06.2021).